Bioorganic & Medicinal Chemistry 17 (2009) 5857–5867

Contents lists available at ScienceDirect

Bioorganic & Medicinal Chemistry

journal homepage: www.elsevier.com/locate/bmc

Free and bound state structures of 6-*O*-methyl homoerythromycins and epitope mapping of their interactions with ribosomes

Predrag Novak [a,*], Jill Barber [b], Ana Čikoš [c], Biljana Arsic [b], Janez Plavec [d], Gorjana Lazarevski [c], Predrag Tepeš [e], Nada Košutić-Hulita [f]

[a] *Department of Chemistry, Faculty of Natural Sciences, University of Zagreb, Horvatovac 102a, HR-10000 Zagreb, Croatia*
[b] *School of Pharmacy and Pharmaceutical Sciences, University of Manchester, Stopford Building, Manchester M13 9PL, UK*
[c] *GSK Research Centre Zagreb Ltd, Prilaz baruna Filipovića 29, HR-10000 Zagreb, Croatia*
[d] *National Institute of Chemistry, Hajdrihova 19, SI-1115 Ljubljana, Slovenia*
[e] *Laboratory for Environmental Geochemistry, Faculty of Geotechnical Engineering, University of Zagreb, Hallerova aleja 7, HR-42000 Varaždin, Croatia*
[f] *PLIVA—Research and Development, Prilaz baruna Filipovića 29, HR-10000 Zagreb, Croatia*

ARTICLE INFO

Article history:
Received 24 November 2008
Revised 26 June 2009
Accepted 5 July 2009
Available online 9 July 2009

Keywords:
Homoerythromycins
Free and ribosome-bound structures
Binding epitopes
NMR and molecular modeling

ABSTRACT

The solution and solid state conformations of several 6-*O*-methyl homoerythromycins **1**–**4** were studied using a combination of X-ray crystallography, NMR spectroscopy and molecular modelling calculations. In the solid state **1** was found to exist as the two independent molecules with similar structures termed 3-*endo*-folded-out. In solution a significant conformational flexibility was noticed especially in the C2 to C5 region. The compounds **1** and **2** unlike 14-membered macrolides adopted the 3-*endo*-folded-out conformation while **3** and **4** existed in the classical folded-out conformation. TrNOESY and STD experiments showed that **1** and **2** bound to the *Escherichia coli* ribosome while **3** and **4**, lacking the cladinose sugar, did not exhibit binding activities, this being in accordance with biochemical data. The bound conformations were found to be very similar to the free ones, some small differences were observed and discussed. The STD experiments provided evidence on binding epitopes. The structural parts of **1** and **2** in close contact with ribosome were similar, however the degree of saturation transfer was higher for **2**. The differences between tr-NOE data and STD enhancements in **1** and **2** arouse as a consequence of structural changes upon binding and a closer proximity of **2** to the ribosome surface. An understanding of the molecular mechanisms involved in the interaction of macrolides with ribosomes can help in developing strategies aiming at design of potential inhibitors.

1. Introduction

Erythromycin and its derivative azithromycin are well-known macrolide antibiotics, effective against Gram-positive and certain Gram-negative microorganisms.[1] Macrolides exert their activity by interacting with bacterial 50S ribosomal subunit at, or close to, the peptidyl-transferase center and thus inhibit the growth of the nascent peptide chain. However, the increasing resistance to ribosome-targeting antibiotics has become a global problem and much effort is now directed toward new and more potent classes of drugs to overcome resistance mechanisms. An effective approach to overcoming this problem is to understand the principles of how these drugs interact with the ribosome.[2] Recently, crystal structures of some ribosome–macrolide complexes[3–7] have thrown new light on the binding mechanisms of macrolides to ribosomes and hence provide a good basis for the rational design of new ligands and inhibitors. However, when analysing solid state structures of ribosome–macrolide complexes one should keep in mind the discrepancies between structures obtained for the halophilic archeon *Haloarcula marismortui*[5] and *Deinococcus radiodurans*.[6] The proposed models differ significantly even though ribosomal 50S subunits of the two bacteria have drug binding sites whose sequences are highly conserved. Furthermore, the crystal structure data obtained so far on complexes of macrolides with ribosome isolated from clinically non-relevant bacteria do not explain all the effects of macrolides on different pathogenic strains. An example would be good here. In spite of the knowledge gained so far on macrolide antibiotics an understanding of the mode of their interactions with ribosome still remain incomplete with many issues unresolved.[8,9] We believe that steps taken in the process of drug design should also include elucidation of the solution state structures of free and bound ligand molecules since the structural features of the complex may not be exactly the same in solution and in the solid state.[7,10]

In our recent papers[11,12] we have shown that a systematic approach which combined NMR and molecular modelling calculation

* Corresponding author. Tel.: +385 14606184; fax: +385 14606181.
E-mail address: p.novak@chem.pmf.hr (P. Novak).

0968-0896/$ - see front matter © 2009 Elsevier Ltd. All rights reserved.
doi:10.1016/j.bmc.2009.07.013

could generally be applicable to conformational studies of macrolides free and bound to ribosomes. Our results,[11–13] as well as those of others,[14–18] demonstrated that macrolides adopt two major conformational families; folded-out and folded-in, referring to the outward and inward folding of the ring fragment C2–C5. The vicinal coupling constants $^3J_{H2H3}$ and NOE proton–proton contacts such as H3–H11 and H4–H11 are good indicators of the aglycone folding.[12] Furthermore, the $^3J_{CH}$ coupling constants over the glycosidic bonds[12,18] might provide information about the position and mobility of the two sugars, (desosamine and cladinose), with respect to the lactone ring. Longitudinal relaxation of methyl protons could be useful to probe motions of methyl groups which reflect the aglycone ring folding.[14,16] Additionally, by applying transferred NOESY (tr-NOESY) and saturation transfer difference (STD) NMR experiments it is possible to characterize binding of macrolides to ribosomes.[11]

In this paper we report on conformational analyses of several 15-membered azalides (Fig. 1), for example, 6-*O*-methyl-9a-aza-9a homoerythromycin A (**1**), 6-*O*-methyl-8a-aza-8a homoerythromycin A (**2**) and their decladinosyl derivatives (**3**) and (**4**). Compounds **1** and **2** are particularly interesting to see whether difference in the position of the lactam group (Fig. 1) has an impact on the overall conformation of the molecules and how this affects the affinity for the ribosome. Binding studies of decladinosyl derivatives **3** and **4** are expected to clarify the observed low activity of 15-membered azalides without the cladinose sugar attached at position 3.

We now report the use of a combination of NMR measurements (coupling constants, NOE and relaxation data) and molecular modelling calculations to determine the solution state structures of **1**–**4** in polar (water) and non-polar (chloroform) media. Variable temperature measurements were also performed to check the conformational stability of the studied molecules. The obtained solution state conformations of **1** were compared to the solid state conformation as determined by X-ray crystallography. Transferred-NOESY and STD (Saturation Transfer Difference) experiments were next employed to asses bound conformations and to characterize interactions of **1**–**4** with *Escherichia coli* ribosomes. Tr-NOESY experiments provide data on the bound conformations of the studied compunds.[19] STD is a promising tool for identification of the binding epitopes of drug–receptor interactions,[10,20,21] information which can further be exploited in the design of molecules with bioactivity. The obtained results have been compared with those found for the related macrolide–ribosome complexes, both in solution[11] and in the solid state.[3–7]

2. Results and discussion

2.1. NMR assignments

The syntheses and chemical shifts of **1**–**4** in $CDCl_3$ were described elsewhere.[22] The complete ^1H and ^{13}C atom assignments in D_2O (see Supplementary data) were made by the combined use of the standard one-dimensional (^1H and APT sequences) and two-dimensional homo- and heteronuclear (COSY, HSQC and HMBC sequences) experiments. The homo-nuclear coupling constants were determined from the high-resolution proton and DQF-COSY spectra (Table 1). Vicinal hetero-nuclear coupling constants over the glycosidic bond (Table 2) were extracted from the multi-site ^{13}C selective experiments followed by polarisation transfer to protons, employing the Hadamard formalism.[23,24] NOE and ROE data were obtained from the two-dimensional NOESY and ROESY spectra (Table 3).

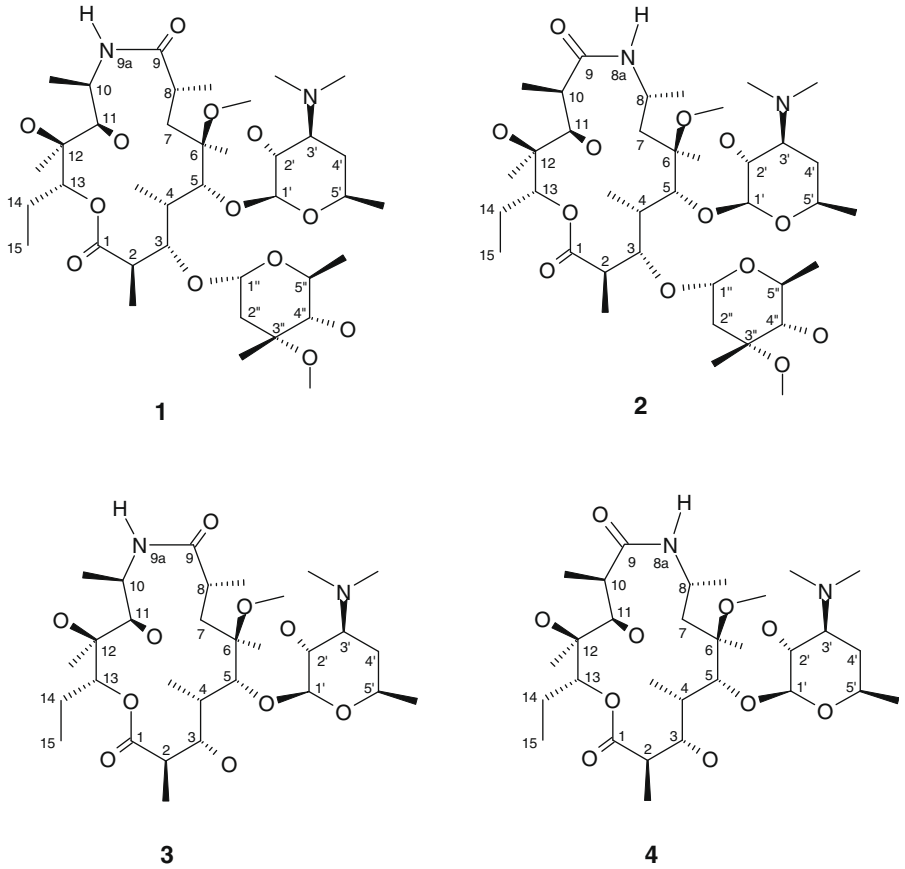

Figure 1. Compounds studied and the atom numbering.

Table 1
Vicinal proton–proton coupling constants $^3J_{HH}$/Hz of compounds **1**–**4** in $CDCl_3$ and D_2O

Protons	1		2		3		4	
	$CDCl_3$	D_2O	$CDCl_3$	D_2O	$CDCl_3$	D_2O	$CDCl_3$	D_2O
H2,H3	5.8	3.6	5.3	4.3	10.1	10.7	10.3	10.7
H3,H4	1.6	1.6	1.2	1.5	Unres.	0.9	Unres.	Unres.
H4,H5	6.8	7.3	7.9	7.3	Unres.	1.5	1.1	1.2
H7a,H8	8.2	10.8	9.2	9.3	5.4	7.0	8.1	8.9
H7b,H8	Unres.	Unres.	2.1	Unres.	2.1	1.5	Unres.	Unres.
H10,H11	Unres.	Unres.	1.4	1.5	1.7	1.8	1.5	Unres.
H13,H14a	1.7	2.2	2.6	2.4	1.6	1.8	2.2	1.1
H13,H14b	10.7	10.6	9.9	10.4	11.0	11.0	10.6	11.0
H1′,H2′	7.2	7.9	7.3	7.6	7.3	7.8	7.3	6.1
H2′,H3′	10.1	10.7	10.7	10.7	10.3	10.5	10.3	10.4
H3′,H4′a	3.8	3.8	Overlap	4.4	3.9	4.9	3.8	4.6
H3′,H4′b	12.4	12.6	12.4	12.2	12.3	12.1	12.3	Overlap
H4′a,H5′	1.7	2.0	2.1	2.0	1.9	1.8	1.8	1.5
H4′b,H5′	10.7	11.0	10.8	11.3	10.8	Overlap	11	Overlap
H1″,H2″a	0.7	Unres.	Unres.	Unres.		—	—	—
H1″,H2″b	4.4	4.9	4.5	4.6		—	—	—
H4″,H5″	9.8	9.8	9.3	9.7		—	—	—

Table 2
Comparison of the vicinal carbon–proton coupling constants $^3J_{C,H}$/Hz over the glycosidic bond obtained from the NMR experiment for compounds **1**, **2** and azithromycin[11] with those calculated from the X-ray for **1**

Atoms	1	2	Azithromycin	1	
	$^3J_{C,H}$ measured			Φ	$^3J_{C,H}$ calcd
H3,C1″	4.6	4.8	2.2	31.2	5.9
C3,H1″	4.6	4.9	4.1	41.2	4.5
H5,C1′	6.6	5.8	6.7	14.4	7.7
C5,H1′	3.7	3.3	3.5	41.8	4.4

2.2. Crystal structure

X-ray structure analysis has shown that in the solid state **1** exists as the two crystallographically independent molecules, **1a** and **1b** with very similar structures (Fig. 2). Each molecule crystallizes with acetone and seven water molecules in an asymmetrical unit. A complex network of hydrogen-bonds involving water molecules and **1a** and **1b** is found, while the acetone molecule is placed in the cavities formed.

Table 4 gives key internuclear distances and torsion angles for **1a** and **1b**, compared with the crystal structure of azithromycin.[25,26] Like compound **1**, azithromycin also forms two very similar structures in the crystalline state.

In both **1a** and **1b** structures the macrocyclic ring of **1** adopts a conformation intermediate between the classical folded-out and folded-in structures, and similar to the azithromycin solution structure. While the Western portion of the ring is folded-out, as reflected by the H8–H11 and H4–H6Me internuclear distances (these are both <4 Å in folded-in conformers), the H3–H11 internuclear distance and the H3–H4 torsion angle are more characteristic of folded-in structures. As we have shown previously,[17] there is considerable torsional freedom in the H2–H5 part of 15-membered macrocyclic rings. On balance therefore, these are folded-out structures, but the term 3-*endo*-folded-out could be used to define the structures more precisely.

The 6OMe group is oriented toward atom C3 in both **1a** and **1b**. The oxygen atom in the lactam group is oriented toward the macrocyclic ring due to the rotation around the C8–C9 bond, with the torsion angle C7–C8–C9–N9 of 135.0° and 134.5° for **1a** and **1b**, respectively. This orientation prevents the formation of the intramolecular hydrogen-bond N9–H9···O6. A slight difference between the two molecules is noticed in the region C13–C2 of the macrocyclic ring with the torsion angles O–C1–C2–C3 and C1–O–C13–C12 of 149.2° and 106.7° for **1a** and 132.9° and 122.5° for **1b**.

The sugar rings adopt chair conformations and their orientation with respect to the macrocycle is defined with the torsion angles C2–C3–O3–C1″, C3–O3–C1″–O6″, C4–C5–O5–C1′ and C5–O5–C1′–O6′ of −90.4, −76.4, −102.3 and −78.3 in **1a** and −85.3, −76.0, −99.6 and −77.3 in **1b**, respectively. The cladinose is almost parallel while desosamine is perpendicular toward the macrocyclic ring. A slight difference in the orientation of the desosamine sugar in **1a** and **1b** is also indicated (Fig. 2).

2.3. Solution state structure

2.3.1. Macrocyclic ring

To determine the conformational characteristics of the 15-membered macrocyclic ring and two sugar units in solution of compounds **1**–**4**, we measured vicinal proton–proton $^3J_{H,H}$ coupling constants in polar and non-polar solvents (Table 1) as well as carbon–proton $^3J_{C,H}$ coupling constants around the glycosidic bonds in **1** and **2** (Table 2). As stated previously[11–13] only the $^3J_{H2,H3}$ coupling constant changed significantly with changing the solvent polarity and raising the temperature.

Table 1 shows vicinal coupling constants obtained for **1**–**4**. The values of $^3J_{H2,H3}$ are immediately striking. Compounds **3** and **4** exhibit large values, suggesting torsion angles of close to 180°; these values are consistent with the classical folded-out conformation. For compounds **1** and **2**, however, $^3J_{H2,H3}$ values in both water and $CDCl_3$ are much smaller, suggesting average torsion angles of only just above 90°. These values are consistent with that obtained in the crystal structure of **1** as shown in Table 4, suggesting that **1** and **2** may form 3-*endo*-folded-out structures, as described for azithromycin.

Further conformational information about the macrocyclic ring can be obtained by NOE or ROE experiments, and these were now used to gain a more complete understanding of the conformational equilibria shown by compounds **1**–**4**. As already observed for the related macrolides,[11,12,17] NOE's are close to zero or change sign in D_2O, and therefore we recorded ROESY spectra of **1**–**4** in buffered solution (as displayed in Fig. 3a for **2**) and NOESY spectra in $CDCl_3$. To suppress the unwanted TOCSY–COSY cross-peaks the T-ROESY sequence[28] was also employed. The observed ROE contacts of **1**–**4** are displayed in Table 3. The H3–H11 and H4–H11 ROE contacts were both observed in buffered solutions of **1** and **2** (Table 3), consistent with the 3-*endo*-folded-out conformation, but also, of course, consistent with folded-in conformers. The absence of H3–H8 and H8–H11 contacts and the presence of H5–H6Me contacts strongly indicate that **1** and **2** adopt 3-*endo*-

Table 3
ROE contacts of compounds **1–4** in D_2O

Atom	ROE			
	1	**2**	**3**	**4**
2	4Me,4,3,11	4Me,4,3,11	4Me,4	4Me,4
2Me	4Me,3	4Me,3,1″	3	3
3	4Me,2Me,4,2,6OMe,11,5,1″	4Me,2Me,4,2,6OMe,11,5,1″	2,2Me,4,5,6OMe	2Me,4,5,6OMe
4	7a,2,11,5,3	7a,2,11,5,3	3,5,7a,11	2,3,5,7a,11
4Me	2Me,2,3″OMe,5,1′	2Me,2,3″OMe 2′,5,1′	2	2,5,7a,11
5	4Me,6Me,5″Me,4,6OMe,3,5″,1′	4Me,6Me,5″Me,4,6OMe,3,5″,1′	3,4,6Me,6OMe	3,4,6Me,6OMe
6Me	4,8,6OMe,5	8,6OMe,5	5,6OMe,8	6OMe,7b,8
6OMe	6Me,8,11,5,3,5″Me,	6Me,8,11,5,3,5″Me,	3,5,6Me	3,4,5,6Me
7a	8Me,7b,4	8Me, 7b, 11,4	4,4Me,8,8Me	4,4Me,5
7b	7a,8,8Me,	7a,8,8Me	6OMe, 8Me	6Me,7a,8
8	7b,6Me,6OMe,8Me	7b,6Me,6OMe,8Me	6Me,6OMe,7a,7b	6Me,7a,7b,8Me
8Me	8,7b,7a	8,7b,7a	7b	6OMe,7a,7b,8
10	10Me,12Me,11	10Me,12Me,11	10Me,11,12Me	11,12Me
10Me	11,10	11,10	10,11	—
11	10Me,12Me,4,2,3,10, 6OMe,13	10Me,12Me,4,2,3,10, 6OMe,13	4,4Me,10,10Me,12 Me,13	4,10,12Me,13
12Me	14b,14a,11,10	14b,14a,11,10,2	11,14a,14b	10,11,14a,14b
13	15,14a,14b,12Me,11	15,14a,12Me,11	—	11,12Me,14a,14b,15
14a	12Me,13,14b	12Me,13,14b	13	13,14b
14b	12Me,14a,13	12Me,14a,13	12Me,15	12Me,14a
15	14b,	13,2Me	13,14b	13,14b
1′	4Me,3′,3″OMe,2′,5,5′,5″	4Me,3′,3″OMe,2′,5,5′,5″	—	4Me,5,6Me,2′,3′,5′
2′	4′b,3′NMe_2	4′b,3′NMe_2,5′	4′b,3′NMe_2,3′	4′b,3′NMe_2
3′	3′NMe_2,5′,1′,4′a	3′NMe_2,5′,1,4′a	2′,3′NMe_2,5′,4′a	3′NMe_2,5′,4′a,4′b
3′NMe_2	4′b,4′a,3′,2′	4′b,4′a,3′,2′	4′b,4′a,3′,2′	4′b,4′a,3′,2′
4′a	4′b,3′NMe_2,5′,5′Me,3′	4′b,3′NMe_2,5′,5′Me,3′	4′b,3′NMe_2,5′,3′	4′b,5′,3′
4′b	4′a,3′NMe_2,2′	4′a,3′NMe_2,2'	4′a,3′NMe_2,2′,5′Me	4′a,2′
5′	5'Me,4′b,4′a,3′,5″,1′	5'Me,4′a,3′,5″,1′	5'Me,4′a,3′	4′a,3′
5′Me	4′a,5′	4′a,4′b,5′	4′a,5′	4′a,5′
1′′	3″Me,2″b,2″a,4″,3	3″Me,2″b,2″a,4″,3,3′′OMe	—	—
2′′a	3″Me,2″b,3″OMe	3″Me,2″b,3″OMe	—	—
2“b	3″Me,2″a,4″,1″	3″Me,2″a,4″,1″	—	—
3″ Me	2″a,2″b,4″,3″OMe,1″	2″a,2″b,4″,5″, 3″OMe,1″	—	—
3″OMe	2″a,3″Me,4Me,5″	2″a,3″Me,4Me,5″	—	—
4″	3″Me,5″Me,2″b,5″	3″Me,5″Me,2″b,5″	—	—
5″	5″Me,4″,5,5′,1′	5″Me,4″,3″OMe,5,5′,1′	—	—
5″Me	4″,5″,6OMe	4″,5″,6OMe,	—	—

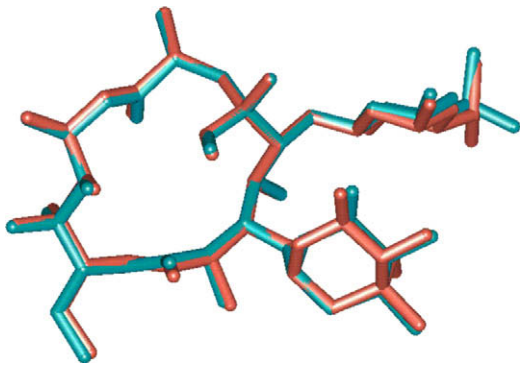

Figure 2. The superposition of the conformations of the two crystallographically independent molecules **1a** and **1b**.

folded-out conformations, however in **1** the H3–H11 cross-peak was stronger than the 4H–11H cross-peak while the opposite was found in **2**, where H4–H11 cross-peak was stronger than H3–H11 (Fig. 3a). Compound **1** also exhibits a weak H4–H6Me cross-peak. This signal is characteristic of the folded-in conformation and suggests that **1** has a greater folded-in character than **2.** Compounds **3** and **4** both exhibited strong NOEs between protons 4 and 11, while no H3–H11 contact was observed in the ROESY spectra. This, together with coupling constant data, strongly supports the conclusion that these compounds adopt the classical folded-out conformation in both D_2O and $CDCl_3$. The absence of the cladinose sugar at position 3 enabled the macrocyclic ring to be more flexible and to adopt the energetically more favoured folded-out conformation.

2.3.2. Sugar rings

The large diaxial coupling constant in cladinose and desosamine (Table 1) reflected the chair conformations[14] of both sugar rings in **1** and **2** and desosamine in **3** and **4**. The observed intra-sugar ROE's (Table 3) are in agreement with this.

Table 4
Key torsion angles and internuclear distances for two crystallographically independent molecules **1a** and **1b** compared with the crystal structure of azithromycin (Azi a and Azi b; data taken from Refs .25,26 is very similar)

	Torsion angles (°)				Internuclear distances (Å)					
	H2,H3	H3,H4	H4,H5	H7s,H8	H3,H8	H3,H11	H4,H11	H4,H6Me	H5,H6Me	H8,H11
1a	112.2	−73.9	144.4	161.4	5.0	3.4	3.5	4.3	2.4	4.3
1b	113.8	−70.5	141.3	160.1	5.1	3.5	3.4	4.3	2.4	4.2
Azi a	111.6	−72.5	141.3	155.6	5.5	3.2	3.5	4.0	2.6	4.8
Azi b	112.3	−67.2	139.5	154.0	5.5	3.1	3.2	4.0	2.6	4.8

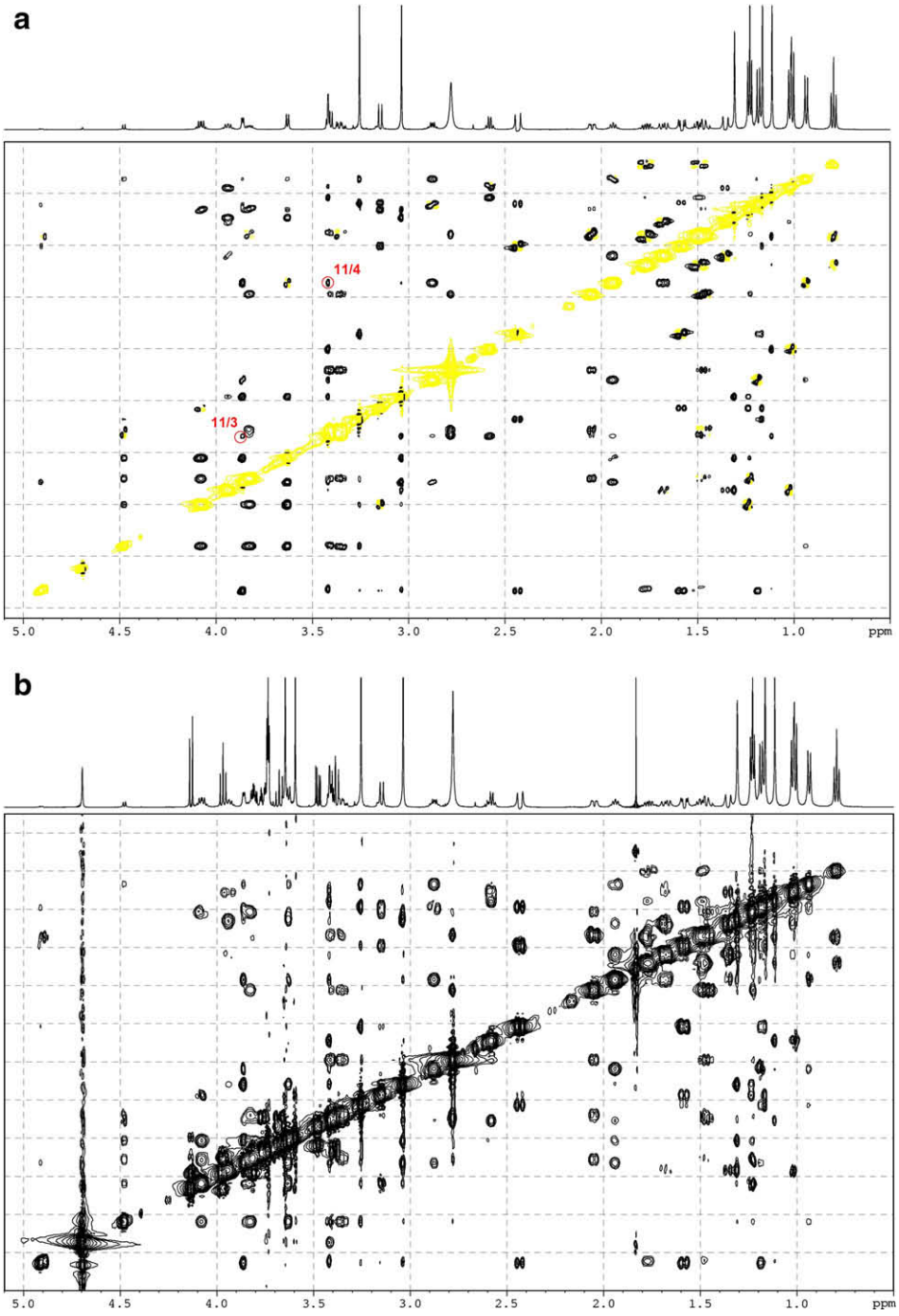

Figure 3. Comparison of (a) the ROESY spectrum and (b) tr-NOESY spectrum of compound **2** after addition of *E. coli* ribosome, both recorded in TRIS buffer at 25 °C (important NOE peaks are indicated in red).

The vicinal carbon–proton coupling constant over the glycosidic bond could be useful to determine the relative position of the sugars with respect to the macrocyclic ring.[12,18] Hence, these coupling constants for **1** and **2** were extracted from the multi-site ^{13}C selective one-dimensional experiments using Hadamard formalism.[23,24] The four simultaneous experiments were used to excite C3, C5, C1′ and C1″ carbon atoms which afforded the determination of $^{3}J_{CH}$ values for **1** and **2** listed in Table 3. $^{3}J_{CH}$ coupling constant over the glycosidic bond are similar to those found for azithromycin and related macrolides,[12] indicating a similar orientation of the sugars.

The H1′–H5 and H1′–H4Me ROE contacts were observed for all compounds, which corresponded to the perpendicular orientation of the desosamine sugar with respect to the macrocycle, being consistent with the X-ray structure of **1** and the data observed for the related macrolides.[12,14–18] On the other hand, a close proximity of H1′ and H5″ and H5–H5″ atoms indicated approximately parallel orientation of the cladinose in compounds **1** and **2** (Table 3) as also observed in the solid state. Inter-sugar contacts H1′–H5′ and H1′–H3″OMe suggest the up–up orientation of the alpha-faces of the two sugars in **1** and **2**.

2.4. The motional properties of methyl groups

Longitudinal relaxation time measurements (T_1) of methyl protons can provide further information about mobility of methyl groups and aglycone ring folding.[14,16] T_1 values were measured in

$CDCl_3$ solution and are given in Table 5. In the 14-membered macrolides, the folded-out and folded-in conformations differ by the position of 4Me and 2Me groups. The folded-out is characterized by a high energy barrier to the rotation of 2Me resulting in a short proton longitudinal relaxation times.[14,16] In the folded-in conformation 2Me group has more motional freedom due to lessening of the restriction to rotation, while the mobility of 4Me is reduced since 4Me is positioned in the more congested environment.

For azithromycin, shorter T_1 values for 4Me than 2Me were observed[16], and this is also true of **1** and **2**, see Table 5. This would be consistent with a folded-in conformation. However, as noted previously, 15-membered macrolides show conformational flexibility around H3–C3–C4–H4 and this will result in increased freedom for 4Me. This result therefore is consistent with a 3-*endo*-folded-out conformation. In the decladinosyl compounds **3** and **4** both 2Me and 4Me rotate freely since there is no steric hindrance imposed by the cladinose, which in turn results in a longer T_1 values (Table 5).

2.5. Molecular modelling

Detailed conformational structures may be constructed from NMR studies combined with molecular modelling in two ways. Either we may carry out unconstrained modelling and then search for low energy conformations that satisfy the NMR data, or we may constrain the modelling calculations to the NMR data. The danger with the first method is that small errors in the assumptions made by the modelling package may lead to incorrect conformations being proposed. The danger with the second method is that averaging of multiple conformations is difficult to recognise.

We carried out unconstrained Monte Carlo searches of both **1** and **2** using both AMBER and MM2 force fields. For **1** the AMBER force field 10 lowest energy structures were characterized by an orientation of the Western half of the macrolides ring such that 11H is *exo* to the ring, giving rise to large distances between 3H and 11H and also 8H and 11H (see Supplementary data). The same pattern was seen using MM2 as the force field, the global minimum being almost identical. Good convergence was seen and no structure within 20 kJ mol^{-1} of the global minimum showed a conventional 11-*endo* conformation.

A similar picture was seen for compound **2**, except that conventional folded-out structures were now found 18 kJ mol^{-1} above the global minimum when the AMBER force-field was used. Lower energy structures were all variations of the 11-*exo*-folded-out conformation. The MM2 force-field also found an 11-*exo* structure with excellent convergence, but it was not identical with the global minimum found using the AMBER force-field. Representative 11-*exo*-folded-out structures are shown in Figure 4, alongside the conventional 11-*endo* conformations.

We investigated the inconsistency between modelling and solution structures in several ways. Firstly, we repeated the modelling studies, this time for compounds **1**–**4**, using molecular dynamics simulations. Initially a range of force-fields and gradient functions were explored using compound **1,** and the Tripos force-field and Powell method were found to give the best (lowest energy) results. The four structures were then heated and cooled in silico, varying the rates of heating and cooling and the highest and lowest temperatures. The energies of the resulting structures were then compared. The results are shown in the Supplementary data.

The lowest energy conformer found for compound **2** was once again an 11-*exo* conformation, as was the second conformer. The third conformation in energy was, however, an 11-*endo* conformation and was only about 4 kcal mol^{-1} higher in energy. Compounds **3** and **4** behaved almost identically with an 11-*endo* conformation energetically higher by about 4 kcal mol^{-1} than the 11-*exo* conformation. For compound **1** an 11-*endo*-folded-in conformation was found at lowest energy.

Although it is well known that it is very difficult to represent aqueous solution accurately in silico, the persistence of the 11-*exo* conformers led us to wonder if they had any basis in reality. Analysis of the 11-*exo* conformers in silico, shows that these conformers are expected to give rise to strong H11–H12Me, H11–H10Me and H7–H2′ cross-peaks. For none of the compounds **1**–**4** do we observe a H7–H2′ cross-peak, although this could be weak because of the multiplicity of the H2′ signal. H11–H10Me is a weak signal in both **1** and **2**. Only H11–H12Me is observed clearly, and this is expected also in 11-*endo* conformers. Therefore, there is no clear evidence of *11-exo* conformers in **1** or **2**.

Finally, constrained Monte Carlo searches were carried out on both **1** and **2**. Key distances dictated by the trNOESY and ROESY spectra were constrained in order to maintain 11-*endo*-conformations with 'up–up' arrangements of the sugars. Using the crystal structure of **1** as the starting point, and deriving a structure for **2** from **1**, the distances H11–H4, H11–H3, H3–H1″, H5–H5″, H1′–H5″, H1′–H17, H1′–H8″, H5′–H5″ were constrained to within 0.5 Å of the starting structure for distances below 3 Å, or to within 1 Å for distances in the range 3–4 Å. The results are summarized in the Supplementary data.

Even after constraining the Monte Carlo search there is poor agreement between the results obtained for different force fields, and the agreement between experiment (NMR) and modelling is not complete. While compound **2** adopts a 3-*endo*-folded-out structure in silico, the ROESY spectrum of this compound shows weak H4–H18 and H3–H11 signals, suggesting trace amounts of the folded-in conformer are also present. For compound **1,** a 3-*endo*-folded-out structure is predicted by the AMBER force-field, but the MM2 force-field prefers a folded-in structure (albeit one in which 8H, constrained by the amide function does not make close contact with 3H or 11H). Again, the NMR data support the dominance of the 3-*endo*-folded-out conformer, but with some folded-in character also present.

Molecular modelling cannot therefore define the structures of these compounds. Rather, it reveals the extreme conformational flexibility of **1** and **2**. Both folded-out and folded-in conformations are available to them, although they prefer 3H to be *endo* to the macrocycle and 8H to be *exo*, resulting in a predominance of the 3-*endo*-folded-out conformation. 11-*exo*-conformers are also expected, although they are not definitely detectable by NMR suggesting that they are present at very low concentrations.

Table 5
Longitudinal relaxation times, T_1/s for aglycone methyl protons in **1**–**4**

Compound Methyl	1	2	3	4
2	0.422	0.478	0.571	0.478
4	0.373	0.377	0.675	0.547
6	0.309	0.366	0.434	0.321
6OMe	0.590	0.658	0.798	0.663
8	0.395	0.380	0.510	Overlap
10	0.410	0.590	0.483	0.490
12	0.475	0.430	0.576	0.430
15	0.680	0.944	0.789	0.663

2.6. Binding studies to ribosomes

The compounds **1**–**4** were further subjected to comparative NOESY and STD experiments in the presence of *E. coli* ribosomes to study bound conformations and to determine structural parts in intimate contact with ribosome. As already mentioned, NOE's in D_2O solution of **1**–**4** were close to zero at 600 MHz, while ROE's were all positive. Upon the addition of *E. coli* ribosomes compounds **1** and **2** displayed transferred NOE's as indicated by

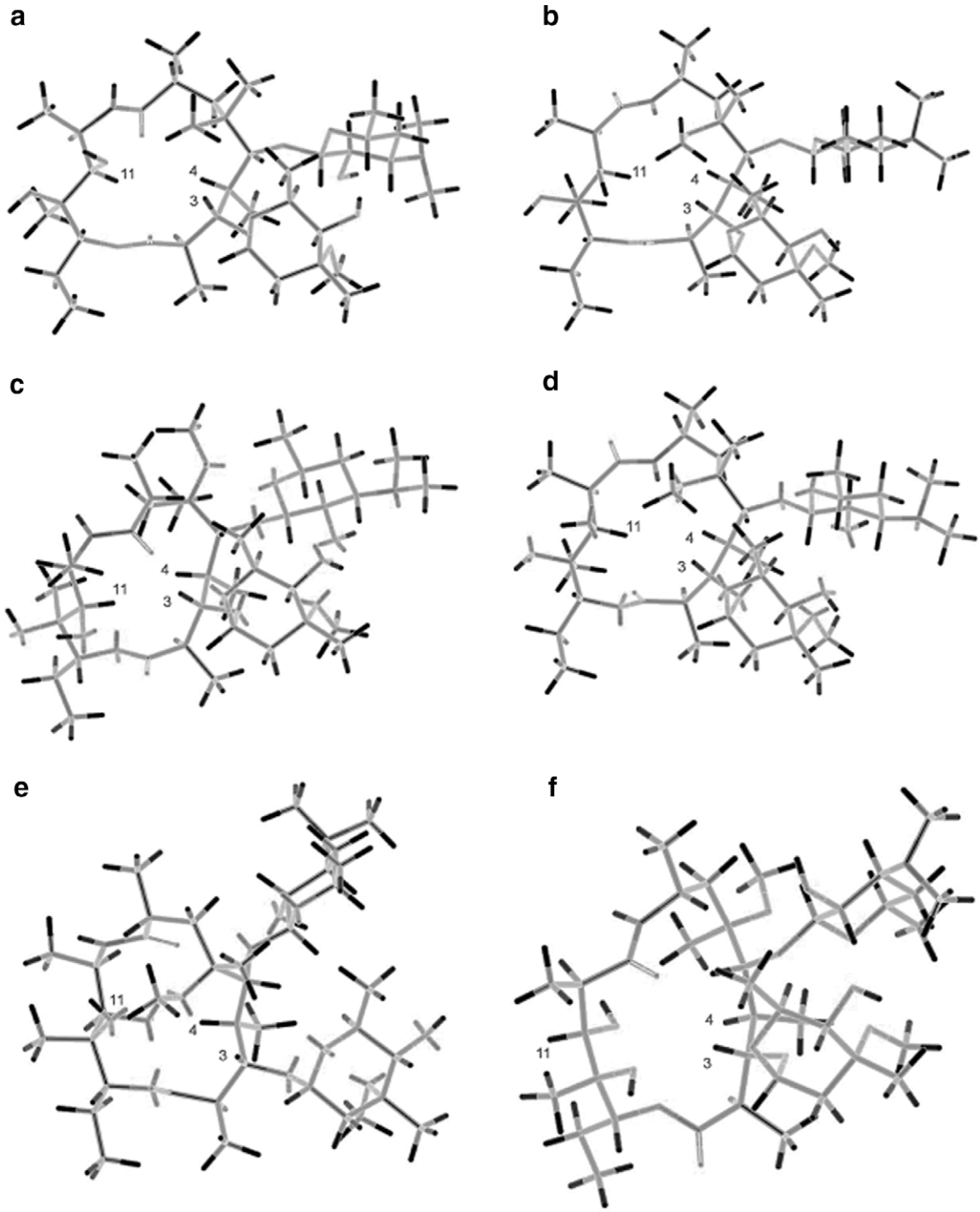

Figure 4. Structures of **1** and **2** found by Monte Carlo conformational searches. Global minima of constrained searches using the AMBER force-field, showing 3-*endo*-folded-out conformers of (a) compound **1** and (b) compound **2**. Global minima of constrained searches using the MM2 force-field, showing (c) folded-in conformation of compound **1** and (d) 3-*endo*-folded-out conformer of compound **2**. Global minima of unconstrained searches using the AMBER force-field showing (e) 11-*exo*-folded-out conformer of compound **1** and (f) 11-*exo*-folded-in conformer of compound **2**.

a negative sign of the cross-peaks (Fig. 3b), corroborating binding to ribosome. Both compounds gave STD spectra as well (Fig. 5) and thus confirmed the binding activity indicated by trNOESY and allowed for the binding epitopes to be determined. On the other hand compounds **3** and **4** exhibited no trNOE signals and displayed very weak STD intensities. This result is consistent with biochemical data which showed that **3** and **4** were inactive against *E. coli*, while **1** and **2** exhibited significant activity (see Table 6).

The features of the trNOESY spectrum of **1** indicate that the bound conformation is very similar to the free one. Namely, all the cross-peaks found in the ROESY spectrum were also found in the trNOESY except for the very weak contact 1″–5″Me. Compared to the free state the compound **2** exhibited several new but also very weak NOE contacts in the bound conformation such as those between protons H7b and H4 in the lactone ring, H5′Me and H3′NMe in the desosamine and between H2″b and H3″OMe in the cladinose. There were also several contacts observed in the

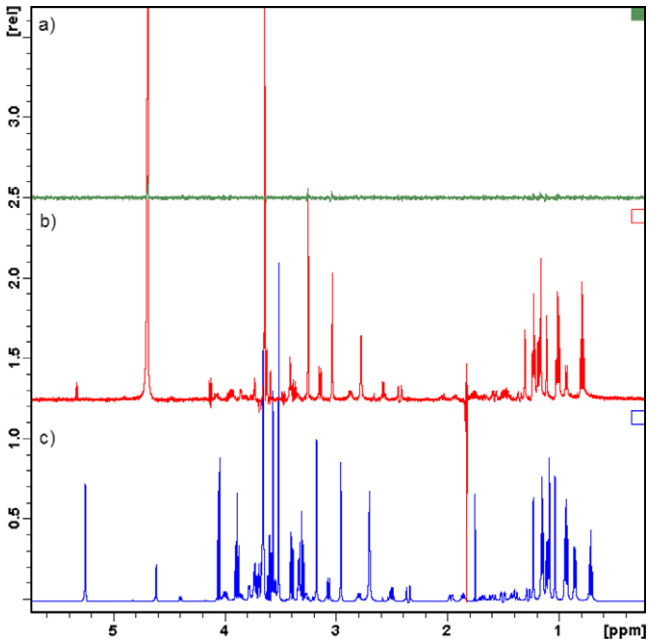

Figure 5. (a) STD-NMR spectrum of **2** prior to addition of the *E. coli* ribosome, (b) STD-NMR spectrum of **2** after addition of the *E. coli* ribosome and (c) proton spectrum of compound **2** after addition of the *E. coli* ribosome, (recorded in TRIS buffer at 25 °C).

ROESY spectrum which were absent in the trNOESY, such as H13–H2, H1″–H5″ and H1″–H4″. These differences point toward the lessening of the conformational flexibility of the ethyl side-chain and sugars as a consequence of motional restrictions imposed by the close proximity of this structural moieties of **2** to the ribosome surface. Slight changes in the Eastern part of the macrocyclic region, indicated by the presence of H7b–H4 contact is in agreement with this. Hence, trNOESY experiments strongly suggest that free and bound conformations are almost identical.

Subsequently, we performed STD experiments to identify the regions of the studied compounds in close contact to ribosome. As already mentioned, only compounds **1** and **2** exhibited significant STD enhancements being stronger in the latter than in the former. The STD enhancements are shown in Figure 6. A saturation transfer in **1** was the most efficient for methyl protons (15Me) in the ethyl side-chain. Appreciable STD enhancements were also observed for dimethylamino protons, and 3″Me and 3″OMe protons of the cladinose. The 2Me and 6OMe, protons were saturated too but to a smaller extent. Similarly, the compound **2** exhibited strongest enhancements for methyl protons in the ethyl side-chain too. 3″Me, 3″OMe, 8Me and 2Me groups were moderately saturated. The methyl protons of the dimethylamino group were also enhanced by the saturation transfer. A comparison between STD effects in **1** and **2** reveals common regions of the two molecules that are in intimate contact with ribosome. These include methyl group at position 15, 3″OMe and 3″Me groups of cladinose and dimethylamino group of desosamine. Therefore compounds **1** and **2** have the same structural parts that exhibited the largest saturation transfer indicating similar binding modes. The only difference is the noticeably higher degree of saturation of 10Me group in **2** suggesting that this part is buried deeper into the ribosome possibly due to H-bond interactions involving the oxygen atom of the lactam group. In azithromycin where no oxygen is present at this position the STD was found to be much smaller (Fig. 8). This finding is in agreement with tr-NOE data.

Table 6
IC_{50}/μM values for compounds **1–4**

Compound	IC_{50} (μM)
1	1.3
2	0.1
3	>100
4	>100
Azithromycin	0.3

In order to differentiate between specific and non-specific interactions we have performed competition STD experiments with azithromycin. Namely, the ribosome is very large particle which may offer many non-specific binding sites for molecules **1** and **2**. Azithromycin is known macrolide antibiotics whose binding has been well characterized by X-ray crystallography,[3–6] NMR spectroscopy[11] and by kinetic studies.[27]

To obtain the best experimental conditions pulse shapes, saturation times, on and off-resonance frequencies and other NMR parameters were varied and tested. After the acquisition of the STD-NMR spectrum of compound **2**, we acquired the STD-NMR spectrum of the mixture of azithromycin and compound **2** under the same experimental conditions (see Section 4). Figure 7 displays the STD-NMR signal of the methyl group 15 in compound **2** (green) overlapped with the corresponding signal in azithromycin (red), as well as both signals in the mixture (blue). It is clearly seen that the intensities of the STD signals in the mixture are much smaller compared to the intensities of STD signals of the individual compounds. This could only be possible if the two compounds compete for the same binding site on the ribosome. The fact that both signals are observed also points toward similar binding constants, both in nano molar region.

Figure 8 shows STD enhancements observed for azithromycin and distances between azithromycin and ribosome as determined for X-ray co-crystallized structure of azithromycin and *H. marismortui*.[5] which are in a good correlation. It is seen that those parts of azithromycin found closest to the ribosome in the co-crystallized structure exhibit the highest magnetization transfer in the complex in solution. A comparison between STD effects in azithromycin and **1** and **2** reveals three common regions in closer proximity to the ribosomal surface, desosamine and cladinose sugars (3″Me and 3″OMe) and methyl group at position 15. This is in agreement with the crystal structure of azithromycin–ribosome complex.[5] Hence, it is likely that macrolides **1** and **2** interact with ribosome in a similar fashion as azithromycin.

The binding epitopes of **1** and **2**, as determined by STD, were mapped onto the calculated lowest energy 3-*endo*-folded-out conformations and are displayed in Figure 9.

3. Conclusion

These results provide further evidence that the 15-membered lactam macrolides have more conformational flexibility than 14-membered macrolides, especially in C2–C5 portion of the molecule. When cladinose is absent they adopt folded-out conformations, but in the presence of cladinose they prefer an intermediate conformation (termed 3-*endo*-folded-out) unavailable to the 14-membered macrolides. The presence of two forms of this structure even in the crystal of **1** reflects the conformational flexibility of these compounds.

The bound conformations of **1** and **2** are very similar to those observed in the free state which is in agreement with the results obtained by the crystallography.[3–7] Three common regions closest to the ribosome were found, desosamine, cladinose and methyl group at position 15. The absence of cladinose sugar in **3** and **4** is the main cause of their inability to bind to the ribosome, as indicated by trNOESY and STD experiments. Azithromycin has some unexpected therapeutic properties, for example, it is a promising anti-malarial

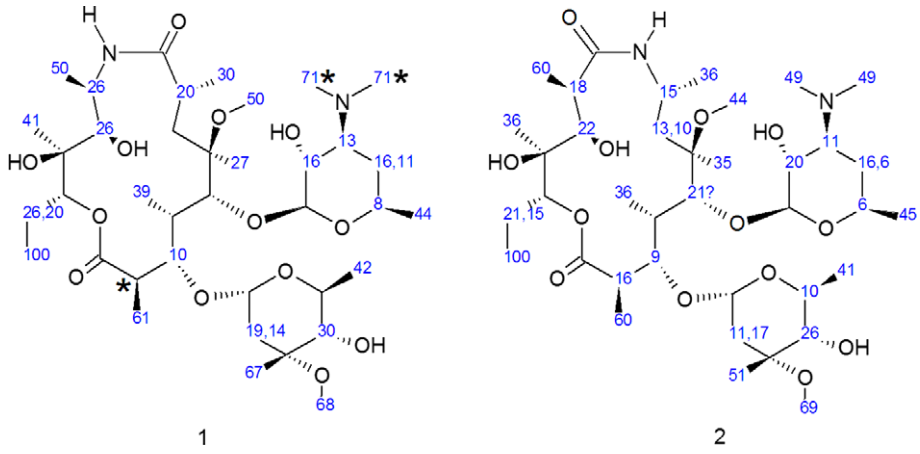

Figure 6. STD enhancements for compounds **1** and **2** (* peak overlap).

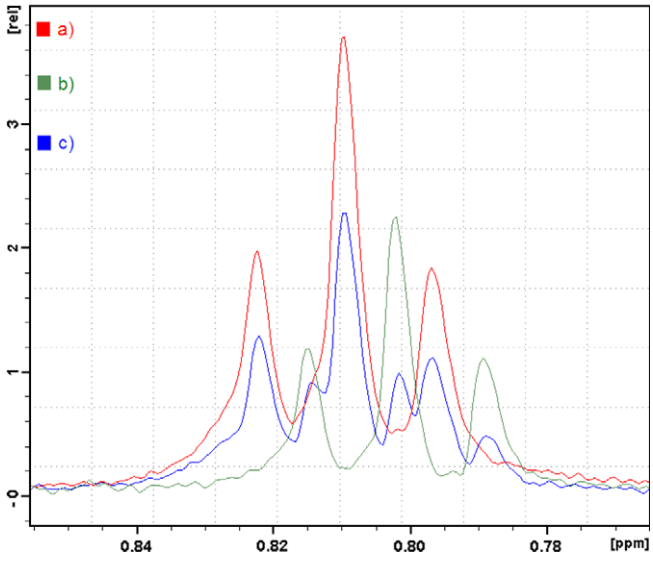

Figure 7. Comparison of STD signal enhancements of atom H15: (a) azithromycin, (b) compound **2** and (c) mixture of azithromycin and compound **2** (all three STD-NMR spectra recorded in presence of the *E. coli* ribosome in TRIS buffer at 25 °C.

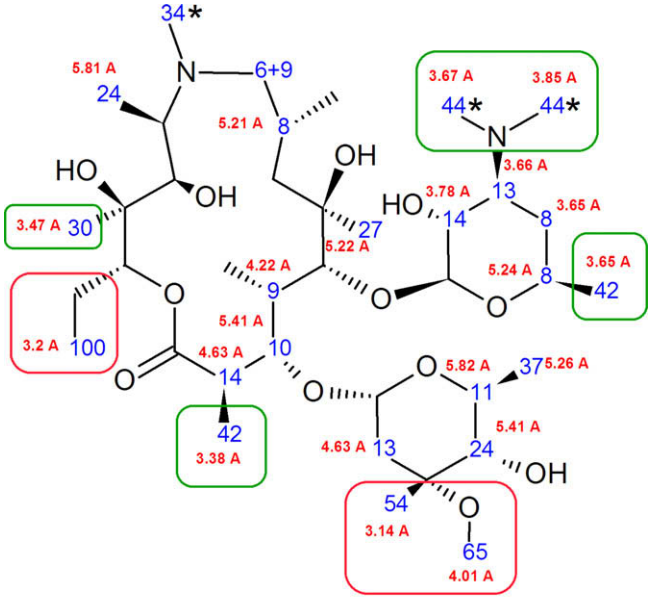

Figure 8. Comparison of STD signal enhancements and distances from ribosome taken from X-ray structure of co-crystallized azithromycin with *H. Marismortui* (* peak overlap).

lead compound,[29] and conformational flexibility, also enjoyed by compounds **1** and **2**, is possibly a contributor to these properties.

4. Experimental

4.1. Sample preparation

Fully deuteriated and non-deuteriated ribosomes were purchased from Dr. Kalju Vanatalu, CDN Ltd, Leete Str. 13, 11313 Tallin, Estonia. Ribosomes were isolated from *E. coli* MRE 600 strain by the zonal ultracentrifuge technique. Deuteriated ribosomes were used for trNOESY experiments, while non-deuteriated were used for STD measurements.

Compounds **1**–**4** were dissolved in buffered D_2O (20 mM TRIS-d_{11}, 60 mM KCl) at pD = 7.4 so that their concentration remains the same for all four compounds (0.003 M). The pH meter reading was adjusted using 0.1 M DCl and 0.1 M NaOD at 0.4 units less than the required value in order to take into account the change in the glass electrode potential because of D_2O.

Ribosomes were added into the solution of **1**–**4** until the final concentration of 8.3×10^{-6} M of ribosome was achieved. The STD and trNOESY experiments were acquired with the total volume of 0.6 ml and the ribosome to macrolide ratio of approximately 1:3500.

4.2. NMR spectroscopy

One and two-dimensional NMR spectra were recorded at 25 °C on Bruker Avance DRX500 and Bruker Avance III 600 spectrometers equipped with 5 mm diameter inverse detection probe with *z*-gradient accessory. In ^1H NMR experiments the spectral width was 10,000 Hz, the number of data points 65 K and the number of scans 8–64. TMS was used as the internal standard. The sample concentration was 10 mg mL^{-1} in $CDCl_3$, acetone-d_6 and DMSO-d_6 solutions and 2 mg mL^{-1} in D_2O and TRIS buffer. The excitation sculpting scheme was used for the water signal suppression. The digital resolution was 0.1 Hz per point.

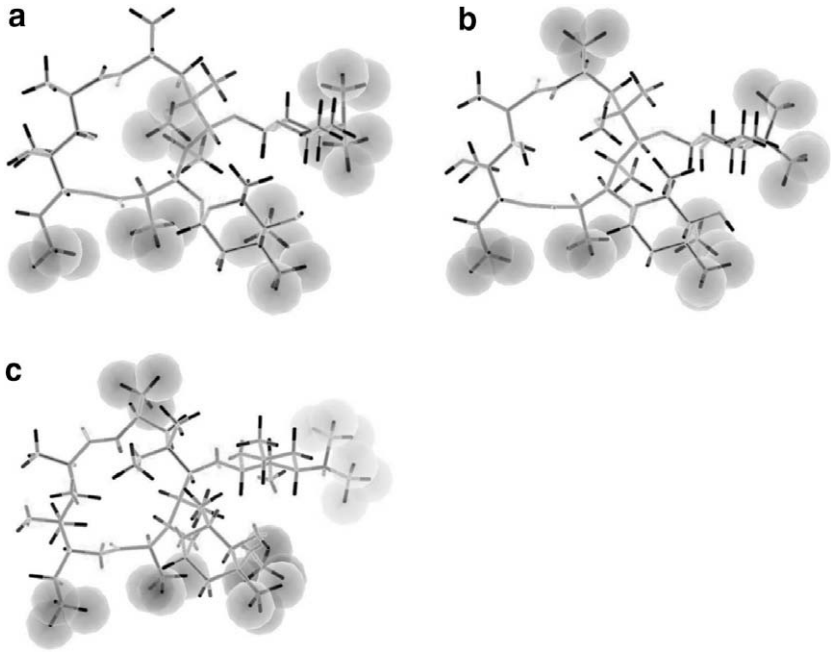

Figure 9. STD binding epitopes of **1** and **2**. (a) STD binding epitope of **1** determined by molecular modelling using AMBER force field and NMR, (b) STD binding epitope of **2** determined by molecular modelling using AMBER force field and NMR and (c) STD binding epitope of **2** determined by molecular modelling using MM2 force field and NMR.

Two-dimensional gCOSY, ROESY and NOESYspectra were recorded under the following conditions: spectral width was 6000 Hz in both dimensions, 2 K data points were applied in time domain and 512 increments were collected for each data set with linear prediction to 1 K and zero filling to 2 K. The number of scans per increment varied between 4 and 32. A relaxation delay was 1.5 s. States-TPPI ROESY spectra were obtained with the mixing time of 250 ms (400 ms for NOESY) and processed with sine squared function shifted by $\pi/2$ in both domains, while gsCOSY spectra were processed with unshifted sine function. The digital resolution was 2.7 and 10.7 Hz per point in $f2$ and $f1$ domains, respectively.

The HSQC and HMBC spectra were recorded with a relaxation delay of 1.5 s and 32 scans per increment. The spectral width was 31,000 Hz in acquisition domain $f2$ and 7500 Hz in time domain $f1$. Data were collected into a 2048 × 512 acquisition matrix and processed using a 2 K × 1 K transformed matrix with zero filling in $f1$ domain. Sine multiplication was performed before Fourier transformations. In HMBC spectra the delay for long-range couplings was set to 60 ms.

Measurements of long-range ^{13}C–^{1}H couplings were performed using the multiple ^{13}C site selective excitation experiment on a Varian Unity Inova 600 spectrometer operating at 600.07 MHz for protons with an inverse detection gradient probe. Half-Gaussian shaped pulse truncated at the leading edge at 5% maximum intensity was used for selective ^{13}C excitation with a duration of 25–50 ms. The relative sign of each selective pulse was set according to the Hadamard matrix. Spectral widths of 4000–5000 Hz were sampled with 32768 data points using 5000 scans for each Hadamard excitation. A BIRD module was used for a better selection of long-range couplings. The two gradients were applied before and after the last pair of 90° pulses for coherence selection and suppression of artefacts.

1D STD-NMR spectra were collected with a 32k data points and a spectral width of 16 ppm by using a sequence provided by Bruker. Selective saturation of the *E. coli* ribosomes was performed using several shaped pulses with varying duration and saturation times to reach the optimum experimental conditions. The Gauss cascade pulse gave the highest sensitivity and selectivity. The saturation time was 3 s. The saturated and reference spectra were acquired and processed simultaneously by creating a pseudo 2D experiment. The saturation frequency was switched from on-resonance (8 ppm) to off-resonance (50 ppm) after each scan. The excitation sculpting scheme was used to suppress the HDO signal.

The trNOESY spectra were acquired using the pulse sequence for phase sensitive 2D homonuclear correlation (*noesygptp19*) provided by Bruker software. Data matrix of 2 K × 512 complex points and 8 scans with sweep width of 5000 Hz was used. Mixing time was 150 ms. Data were zero filled in $f1$ to 1 K and transformed using sine squared function, giving the digital resolution of 2.44 Hz in $f2$ and 4.88 Hz in $f1$ dimension. The excitation sculpting and WATERGATE schemes were used to suppress the HDO signal.

T_1 proton relaxation time measurements were performed on a Bruker Avance DRX500 spectrometer at 500 MHz using the inversion recovery sequence and analyzed by the three parameter fit procedure. 10 τ values in the range 15 ms–4 s were used and the delay was set to five times the longest T_1 value for each compound. The solvent was $CDCl_3$.

4.3. X-ray crystallography

The details of crystal data collection and refinement parameters for **1** are listed in Table 8. Single crystals of the **1** were grown by evaporation from acetone/water solution (1:1, v/v). A colorless needle with dimension 0.6 × 0.2 × 0.2 mm was used for X-ray measurements. Data were collected at 170 K with a Kappa-CCD Nonius diffractometer using graphite monochromated Mo Kα radiation. Data reduction was carried out using DENZO and SCALEPACK[30] software.

The structure was solved by direct methods implemented in SHELXS97[31] and refined by a full-matrix least-squares method based on F^2 using SHELXL97.[31] Hydrogen atoms were positioned geometrically at calculated positions and allowed to ride on their parent atoms. Hydrogen atoms belonging to water molecules are found in different Fourier map and refined isotropically. The refinement converged to R = 4.25%, and wR = 9.01%. The maximum and mini-

mum residual electron densities were 0.02 and −0.01 eÅ^{-3}, respectively.

4.4. Molecular modelling

Compounds **1**, **2**, **3** and **4** were constructed from the crystal structure of compound **1** using Macromodel software.[32] The structures were minimized using the Truncated Newton Conjugate Gradient (TNCG) method[33] in order to obtain local minima.

The Monte Carlo Multiple Minimum (MCMM) conformational search was used to find the global minima.[34] The TNCG method was used as the minimization procedure. A water solvation option using the GB/SA model[35] was used for calculations in water. The search was set to 10,000 structures to be minimized and all structures within 20 kJ mol^{-1} energy range were stored.

Molecular dynamics simulations for compounds **1–4** were performed in SYBYL 7.3[36] Initial structures obtained by change of X-ray crystal structure of dirithromycin were minimized using Tripos force field.[37] Molecular dynamics analysis was completed using SYBYL 7.3 Starting structures were unconstrained and energy minimized using the Tripos force field. The applied atomic charges were Gasteiger-Huckel. The number of iterations was 10,000 and the calculation was terminated when the difference in energy between two conformations was no more than 0.005 kcal/mol.

Acknowledgements

This study was supported by the Ministry of Science, Education and Sports of the Republic of Croatia (Project No. 119-1191342-1083). We are indebted to Dr. S. Koštrun and I. Tatić for helpful discussions and M. Banjanac for performing biochemical measurements.

Supplementary data

Supplementary data associated with this article can be found, in the online version, at doi:10.1016/j.bmc.2009.07.013.

References and notes

1. Schönfeld, W.; Mutak, S. In *Macrolide Antibiotics*; Schönfeld, W., Kirst, H. A., Eds.; Birkhäuser Verlag: Basel, 2002; pp 73–95.
2. Gaynor, M.; Mankin, A. S. *Front. Med. Chem.* **2005**, *2*, 21.
3. Ban, N.; Nissen, P.; Hansen, J.; Moore, P. B.; Steiz, T. A. *Science* **2000**, *289*, 905.
4. Schlünzen, F.; Zarivach, R.; Harms, J.; Bashan, A.; Tocilj, A.; Albrecht, R.; Yonath, A.; Franceschi, F. *Nature* **2001**, *413*, 814.
5. Hansen, J. L.; Ippolito, J. A.; Ban, N.; Nissen, P.; Moore, P. B.; Steitz, T. A. *Mol. Cell* **2002**, *10*, 117.
6. Schlünzen, F.; Harms, J. M.; Franceschi, F.; Hansen, H. A. S.; Bartels, H.; Zarivach, R.; Yonath, A. *Structure* **2003**, *11*, 329.
7. Tu, D.; Blaha, G.; Moore, P. B.; Steitz, T. A. *Cell* **2005**, *121*, 257.
8. Mankin, A. S. *Curr. Opin. Microbiol.* **2008**, *11*, 414.
9. Poehlsgaard, J.; Douthwaite, S. *Nat. Rev. Microbiol.* **2005**, *3*, 870.
10. Johnson, M. A.; Pinto, B. M. *Bioorg. Med. Chem.* **2004**, *12*, 295.
11. Novak, P.; Tatić, I.; Tepeš, P.; Koštrun, S.; Barber, J. *J. Phys. Chem. A* **2006**, *110*, 572.
12. Novak, P.; Banić Tomišić, Z.; Tepeš, P.; Lazarevski, G.; Plavec, J.; Turkalj, G. *Org. Biomol. Chem.* **2005**, *3*, 39.
13. Košutić-Hulita, N.; Matak-Vinković, D.; Vinković, M.; Novak, P.; Kobrehel, G.; Lazarevski, G. *Croat. Chem. Acta* **2001**, *74*, 327.
14. Everett, J. R.; Tyler, J. W. *J. Chem. Soc., Perkin Trans. 2* **1987**, 1659.
15. Steinmetz, W. E.; Shapiro, B. L.; Roberts, J. J. *J. Med. Chem.* **2002**, *45*, 4899.
16. Lazarevski, G.; Vinković, M.; Kobrehel, G.; Đokić, S.; Metelko, B.; Vikić-Topić, D. *Tetrahedron* **1993**, *49*, 72.
17. Awan, A.; Brennan, R. J.; Regan, A. C.; Barber, J. *J. Chem. Soc., Perkin Trans. 2* **2000**, 1645.
18. Bertho, G.; Gharbi-Benarous, J.; Delaforge, M.; Lang, C.; Parent, A.; Girault, J. P. *J. Med. Chem.* **1998**, *41*, 3373.
19. Gyi, J. I.; Pye, D. A.; Barber, J. *J. Chem. Soc., Chem. Commun.* **1991**, 1471.
20. Mayer, M.; Meyer, B. *J. Am. Chem. Soc.* **2001**, *123*, 6108.
21. Vogtherr, M.; Peters, T. *J. Am. Chem. Soc.* **2000**, *122*, 6093.
22. Alihodžić, S.; Fajdetić, A.; Kobrehel, G.; Lazarevski, G.; Mutak, S.; Pavlović, D.; Štimac, V.; Čipčić, H.; Dominis Kramarić, M.; Eraković, V.; Hesenhorl, A.; Maršić, N.; Schoenfeld, W. *J. Antibiot.* **2006**, *59*, 753.
23. Kupče, E.; Freeman, R. *J. Magn. Reson., Ser. A* **1993**, *105*, 310.
24. Blechta, V.; Rio-Portillas, F.; Freeman, R. *Magn. Reson. Chem.* **1994**, *32*, 134.
25. Montejo-Bernardo, J. M.; Garcia-Granda, S.; Bayod-Jasanada, M. S.; Llavota-Diaz, L.; Llorente, I. *Zeitschrift für Kristallographie* **2003**, *218*, 703.
26. Montejo-Bernardo, J. M.; Garcia-Granda, S.; Bayod-Jasanada, M. S.; Llavota-Diaz, L.; Llorente, I. *Zeitschrift für Kristallographie* **2005**, *220*, 66.
27. Petropoulos, A. D.; Kouvela, E. C.; Starosta, A. L.; Wilson, D. N.; Dinos, G. P.; Kalpaxis, D. *J. Mol. Biol.* **2009**, *385*, 1179.
28. Hwang, T.-L.; Shaka, A. K. *J. Am. Chem. Soc.* **1992**, *114*, 3157.
29. Sadiq, S. T.; Glasgow, K. V.; Drakeley, C. J.; Muller, O.; Greenwood, B. M.; Mabey, D. C. W.; Bailey, R. L. *Lancet* **1995**, *346*, 881.
30. Otwinowski, Z.; Minor, W.. In *Macromolecular Crystallography*; Carter, C. W., Jr., Sweet, R. M., Eds.; Academic Press: New York, 1997; Vol. 276, pp 307–326. Part A.
31. Sheldrick, G. M. SHELXS*97 and* SHELXL*97*; University of Göttingen: Germany, 1997.
32. Mohamadi, F.; Richards, N. G. J.; Guida, W. C.; Liskamp, R.; Lipton, M.; Caufield, C.; Chang, G.; Hendrickson, T.; Still, W. C. *J. Comput. Chem.* **1990**, *11*, 440.
33. Ponder, J. W.; Richards, F. M. *J. Comput. Chem.* **1987**, *8*, 1016.
34. Saunders, M.; Houk, K. N.; Wu, Y. D.; Still, W. C.; Lipton, M.; Chang, G.; Guida, N. C. *J. Am. Chem. Soc.* **1990**, *112*, 1419.
35. Still, W. C.; Tempczyk, A.; Hawley, R. C.; Hendrickson, T. *J. Am. Chem. Soc.* **1990**, *112*, 6127.
36. SYBYL 7.3, Tripos Associates, 1699 S. Hanley Road, Suite 303, St. Louis, MO, 2006, 63144-2917.
37. Clark, M.; Cramer, R. D., III; Van Opdenbosch, N. *J. Comput. Chem.* **1989**, *10*, 982.